Geophys. J. Int. (2004) **159,** 1–8 doi: 10.1111/j.1365-246X.2004.02364.x

Gravity-enhanced representation of measured geoid undulations using equivalent sources

Fernando Guspí, Antonio Introcaso and Beatriz Introcaso

Grupo Geofísica, Instituto de Física Rosario, Universidad Nacional de Rosario, Av. Pellegrini 250, 2000 *Rosario, Argentina.*
E-mails: guspi@fceia.unr.edu.ar; geofisic@fceia.unr.edu.ar

Accepted 2004 April 22. Received 2004 April 15; in original form 2003 January 6

SUMMARY

Direct Global Positioning System measurement of geoid undulations on accurately levelled stations, usually tens of kilometres apart, can be interpolated by taking advantage of denser surveys of free-air gravity anomalies covering the same area. Using either a spherical or a planar earth model, a two-layer equivalent source is constructed, with the deepest masses located under the geoid stations and the shallower ones under the gravity stations, in such a way that the effect of the masses fits simultaneously, with different precisions, the anomalous potential related to the geoid and its vertical gradient or gravity anomaly. This poses a linear Bayesian problem, whose associated system of equations can be solved directly or by iterative procedures.

The ability of the described method to predict the geoid elevation over the gravity stations is assessed in a synthetic example; and in the application to a real case, a gravity-enhanced geoid is mapped for an area of Buenos Aires province, Argentina, where local features are put in evidence.

Key words: Bayesian problem, equivalent sources, free-air anomaly, geoid, mapping, physical geodesy.

INTRODUCTION

Satellite technology, using the Global Positioning System (GPS), has greatly improved the determination of Earth's shape, in such a way that the elevation h of a given point over a reference ellipsoid can be measured to within an accuracy of a few centimetres. If a high-precision land survey provides the height H of the same point with respect to sea level, which represents the geoid surface, the difference $h - H$ is a direct measurement of the geoid undulation at that point. Usually, observational stations are placed at the nodes of high-precision levelling networks, located some tens of kilometres apart, so that a regional geoid representation can be obtained. However, when a finer network of gravity measurements, particularly of free-air anomalies, covers the area, this additional amount of information can be incorporated in order to solve the local undulations of the geoid.

When no GPS measurements are available the usual procedure for obtaining a gravimetric geoid involves the integration of the free-air anomalies via Stokes' formula, in order to compute high-frequency corrections to an existing geopotential model such as EGM96 (Lemoine *et al.* 1998) whose wavelength resolution is about 30 arcmin. In this process, the remove–restore technique (Schwarz *et al.* 1990) helps to separate the long-wavelength effect. It should be noted that the values provided by the geopotential model are not considered exact, but a background into which the Stokes' corrections are incorporated.

The picture changes when the geoidal heights are directly measured, because in this case they can be regarded as 'exact data', within their standard errors, and hence a procedure is needed not for integrating the geoid but for filling in the gaps between measurements. This is a situation where the intervening free-air gravity anomalies are able to provide valuable information.

Collocation methods (Moritz 1980; Lahmeyer 1988; Torge 2001) are the classical solution to many interpolation problems in geodesy. They demand much computational time, but their advantage is their flexibility in estimating any kind of gravity field quantity from different types of gravity field observations, including geoid determinations. However, in order to describe the correlation between heterogeneous gravity field quantities, a good knowledge of at least a basic covariance function, such as the covariance of the disturbing potential, is required. It should be transformed into an appropriate model covariance function and applied to other observed quantities using propagation functionals. Remove–restore techniques are generally used, and applications of the collocation method to local and regional geoid determination can be found in Arabelos & Tscherning (1998) and Antunes & Catalao (2000), among others.

Fast Fourier transform (FFT) techniques (Schwarz *et al.* 1990) are able to provide rapid solutions on a flat earth, or with adaptations on a curved earth (Tscherning *et al.* 1994), but they require the data to be gridded prior to the processing, with a consequent loss of accuracy. A finite-difference scheme, using measured

torsion-balance gravity gradients instead of gravity anomalies, has been developed by Volgyesi (2001).

The equivalent-source technique, which has a long tradition in geophysical applications (Dampney 1969; Hansen & Miyazaki 1984; Guspí 1991; Cordell 1992), is historically known in geodesy as the 'buried masses technique' (Balmino 1972); it is known to be unstable and to require regularization. Hauck & Lelgemann (1984) combined buried masses with collocation, and more recent applications of the technique to compute geoid anomalies can be found in, among others, Lehmann (1993) and Antunes & Catalao (2000).

In this paper we develop a variant of the equivalent-source method for the joint representation of different functionals (geoidal height and gravity), where the regularization is achieved using Bayesian statistics. The well-known ambiguity underlying the interpretation of the sources of a potential field is turned into an advantage due to the theoretical fact that outside the causative masses, the potential field is uniquely determined by its values on a reference plane or surface. Thus, if a chosen source (i.e. composed of point masses) is able to generate the field on a surface, it is also able to generate all the transformations, derivatives and continuations of the field. Moreover, the equivalent source can be referred to either a planar or a spherical model without further increasing complexity in the calculations. This paper constructs an equivalent point-mass source whose effect fits simultaneously a potential field (the anomalous gravitational potential related to the geoidal height), and its first vertical derivative (the free-air gravity anomaly). It must be noted that these fields are not independent provided that the derivative field is uniquely determined by the potential. Then, if both fields were given at a set of stations very close together it would pose a problem of compatibility, and noise in the measurements or corrections would be greatly amplified. In the case of this research, however, there are many more gravity anomalies than geoid undulations, and a source is sought that fits both measurements within their standard errors. Long-wavelength anomalies are associated with the geoid measurements and short-wavelength anomalies with the intervening gravity effect; this fact is reflected in the position selected for the point-mass sources.

THEORETICAL MODELS CONSIDERED

We follow Molodensky's theory (Heiskanen & Moritz 1967; Ockendon & Turcotte 1977; Li & Goetze 2001), and in order to define the geoidal height or geoid undulation at any point of the reference ellipsoid, let V be the outer gravitational potential of the Earth, downward-continued to the ellipsoid surface, without consideration of the existing topographic masses, and let V' be the potential due to the ellipsoid at the same point. Then, $V - V'$ is the disturbing potential and, according to Bruns' formula,

$$N = \frac{V - V'}{\gamma} \tag{1}$$

is the geoidal undulation at this point, where γ is the normal gravity (i.e. 980 Gal). Thus, the point of application of the geoid undulation is at ellipsoid level. Heiskanen & Moritz (1967, p. 292) point out the difference between geoidal undulation and height anomaly, yet they closely correspond and differ very little. Moreover, provided the potential of the geoid itself is small compared with that of the topography, it can be included in the indirect effects described by Li & Goetze (2001), so that the geoid height can be considered as referred to sea level.

On the other hand, free-air gravity anomalies are the difference between measured gravity on the Earth's surface and the normal gravity over the ellipsoid at the same geographical coordinates, upward-continued to the topographic level, without including the effect of the topographic masses. It is clear, then, that the point of application of those anomalies is at the topographic level (Levallois 1962; Li & Goetze 2001).

This means that both the disturbing potential and free-air anomalies are the differences of the effect of the same masses: on one hand the mass of the whole real Earth, including topography, and on the other hand the mass of the reference ellipsoid. As has been pointed out, however, the points of application of the observations differ, because in the case of the geoid the outer potential is downward-continued to reference level and in the case of the free-air anomaly the effect of the ellipsoid is upward-continued. Anyway, the causative masses being the same, the combination of geoid heights and free-air anomalies can also be generated by any set of equivalent sources, the gravity anomaly being the vertical derivative of the potential, so that both sets of anomalies can be transformed one into another and handled together without density assumptions (Gleason 1990).

In order to take into account the curvature of the Earth on a surveyed area, the reference sea level surface is represented by an Earth-concentric sphere of mean Earth radius R, in such a way that every point is defined by its geographical coordinates: λ longitude, φ latitude, and elevation or depth ζ respect to sea level (positive downward), $r = R - \zeta$ being the radial coordinate of the point. However, the calculation of the potential and gravity effect of a set of masses is better performed using rectangular coordinates. So, a Cartesian geocentric system is defined (Fig. 1), with the z-axis passing through the poles and the x-axis on the equatorial plane, at the 0° or other reference meridian. The classical formulae of transformation

$$\begin{aligned} x &= r\cos\varphi\cos\lambda \\ y &= r\cos\varphi\sin\lambda \\ z &= r\sin\varphi, \end{aligned} \tag{2}$$

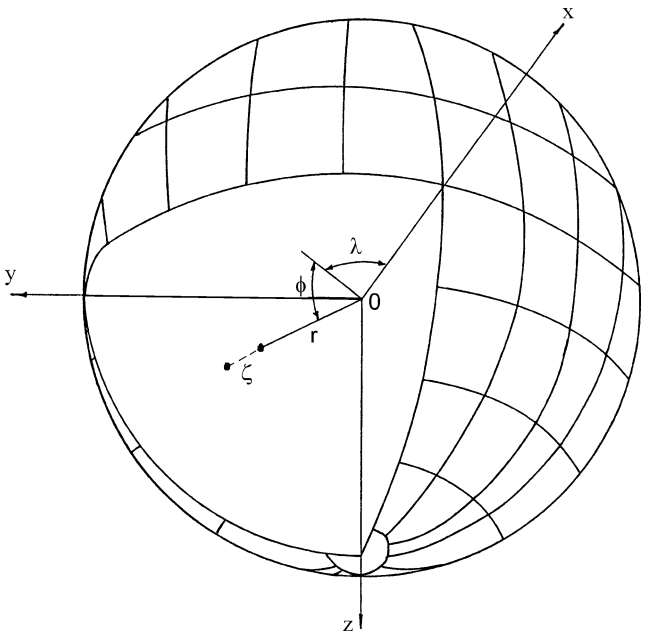

Figure 1. Coordinates on a spherical earth model.

with the direction cosines of the inward-directed radial vector expressed as

$$\mathbf{r} = \left(-\frac{x}{r}, -\frac{y}{r}, -\frac{z}{r} \right), \tag{3}$$

are applied every time they are required.

THE EQUIVALENT-SOURCE TECHNIQUE

Among diverse implementations of the equivalent-source technique mentioned above, we consider that of Cordell (1992). He developed an equivalent-source method for gridding and reducing to a common level a potential field whose values are known on a discrete set of unevenly spaced stations at different altitudes, where a generalized point source is located under each of them. The functional relationship between sources and observations has the form of a Newtonian (or gravitational) potential, and can be applied to any discrete set of potential field data regardless of its nature (gravimetric, magnetic, etc.), in as much as the calculated field from the sources satisfies Laplace's equation and vanishes at infinity. Recognizing that optimum equivalent-source depth and data density are related, the source depth under a given point is chosen proportional to the distance between it and its nearest neighbour.

A generalization of this criterion will be applied to our work. We have two sets of stations: a sparser set of p geoidal heights or potential measurements, whose point of application is considered to be at zero level, as explained above, and a denser set of n free-air gravity measurements, whose point of application is at the physical surface. Considering that the geoid-measured points define a background to which shorter-wavelength contributions are to be added, the depth of the sources within each set is defined as proportional to the distance to the nearest neighbour of the same set. This means that, as a rule, sources under the geoid-observed points will be deeper than those under the gravity stations. An eventual coincidence of both types of sources along the same vertical will put them at different levels. Even the proportionality coefficients may not be the same for both sets of stations, and may be chosen in order to increase the depth differences, as will be illustrated in the examples.

The gravitational potential generated by the whole ensemble of sources should fit the gravitational potential at the measured geoid points, so that the point masses represent physical masses. At the same time, the gravity effect of those masses should fit the values measured at the gravity stations. In a curved earth model, the gravitational potential is always a potential field, but not the gravity anomaly, which is the derivative of the disturbing potential with respect to a variable vertical (radial) direction. In order to keep the potential–gradient relation between both fields, we do not perform remove–restore modifications, the only exception being the possible removal of the mean value of the potential. In a flat earth model, this removal has no effect on the gradients, but in a spherical earth it requires the removal of a small constant quantity from the gravity field too. Of course, if any arbitrary constant is removed from the gravity field only, the potential–gradient relation no longer holds.

THE BAYESIAN PROBLEM

GPS geoid undulations, as well as land gravity anomalies, are all measured within standard errors, and assuming a Gaussian distribution of those errors their variances represent a measure of the most probable distribution of the data around the true values. In Bayesian terms, the knowledge about standard errors, which are different for geoid and gravity measurements, is *a priori* information about data probability. Since our goal is to construct a source model whose effect fits the data within their variances, an infinity of solutions may arise. In order to regularize such a situation, the Bayesian criterion (i.e. Zeyen & Pous 1991; Ulrych *et al.* 2001) also assigns an *a priori* distribution of probability to the model parameters (i.e. the most probable model is that closest to an initial one), in such a way that the solution sought should maximize the probability of the *a posteriori* distribution, that is the joint probability of having the most probable model with the most probable fit to the data. The *a priori* distribution of the model parameters enhances some chosen feature. For instance, the most probable model obtained using a Cauchy *a priori* distribution is sparse (Sacchi & Ulrych 1996; Guspí & Introcaso 2000), and the solution is attained through the iterative resolution of a nonlinear system. In the present problem, we shall only impose a flatness constraint to the model parameters in order to prevent or damp large oscillations (Xia & Sprowl 1991), and this is achieved by assuming they are Gaussian-distributed (Sacchi & Ulrych 1996). Under this hypothesis, the problem can be solved with the single linear system of equations described later in eq. (11).

Let

$$\boldsymbol{\eta} = (\eta_1, \eta_2, \ldots, \eta_p)^{\mathrm{T}}$$

be the vector of measured geoidal heights, and let σ_η^2 be the variance of their measurement errors.

In the same way, let

$$\mathbf{g} = (g_1, g_2, \ldots, g_n)^{\mathrm{T}}$$

be the vector of measured gravity anomalies with error variance σ_g^2.

Let us define the variance ratio $\mu^2 = \sigma_\eta^2/\sigma_g^2$, and the combined data vector

$$\mathbf{d} = (\eta_1, \eta_2, \ldots, \eta_p, \mu g_1, \mu g_2, \ldots, \mu g_n)^{\mathrm{T}}$$

of $m = p + n$ components.

Let

$$\mathbf{c} = (c_1, c_2, \ldots, c_m)$$

be the model parameter vector, where c_i represents a point mass of a Gaussian set whose *a priori* variance is σ_c^2. The number of point masses is m, provided that each of them is located under a measurement station.

The perturbation of the geoidal height at station i due to a unit mass at the place of c_j is expressed as

$$a_{ij} = \frac{G}{\gamma l_{ij}} \tag{4}$$

where G is Newton's constant and $l_{ij} = |\mathbf{l}_{ji}|$ is distance. The vertical (radial) gravity component produced by the same unit mass at the station k is given by

$$a_{kj} = -G \frac{\mathbf{l}_{kj} \cdot \mathbf{r}}{l_{kj}^{3/2}}. \tag{5}$$

In a planar model, only the vertical component is necessary. The coefficients given by eqs (4) and (5) are arranged into an $m \times m$ matrix

$$\mathbf{A} = \begin{pmatrix} \mathbf{A}_\eta \\ \mu \mathbf{A}_g \end{pmatrix} \tag{6}$$

where the submatrix $\mathbf{A}_\eta$ of p rows, contains the coefficients related to the geoid observations, and $\mathbf{A}_g$ contains those of gravity, for convenience scaled by μ. Then

$$\mathbf{d} = \mathbf{A}\mathbf{c} \tag{7}$$

represents the effect of the source on the stations considered.

Although system (7), of order $m \times m$, can be solved directly, its ill-posed nature, discussed in the introduction, requires the *a priori* information to be incorporated in order to solve the Bayesian problem. Thus, we need to minimize the object function

$$S = \frac{1}{2\sigma_c^2}\|\mathbf{c}\|^2 + \frac{1}{2\sigma_\eta^2}\|\boldsymbol{\eta} - \mathbf{A}_\eta\mathbf{c}\|^2 + \frac{1}{2\sigma_g^2}\|\mathbf{g} - \mathbf{A}_g\mathbf{c}\|^2 \tag{8}$$

where $\|\cdot\|^2$ represents the sum of the squares of the components of a vector. In other terms, minimize

$$S = \frac{1}{2\sigma_c^2}\mathbf{c}^{\mathrm{T}}\mathbf{c} + \frac{1}{2\sigma_\eta^2}(\boldsymbol{\eta} - \mathbf{A}_\eta\mathbf{c})^{\mathrm{T}}(\boldsymbol{\eta} - \mathbf{A}_\eta\mathbf{c}) + \frac{1}{2\sigma_g^2}(\mathbf{g} - \mathbf{A}_g\mathbf{c})^{\mathrm{T}}(\mathbf{g} - \mathbf{A}_g\mathbf{c}). \tag{9}$$

Setting $\alpha^2 = \sigma_\eta^2/\sigma_c^2$, multiplying eq. (9) by $2\sigma_\eta^2$, and taking into account the definition of $\mathbf{A}$ from eq. (6) we obtain:

$$\begin{aligned} S &= \alpha^2\mathbf{c}^{\mathrm{T}}\mathbf{c} + (\boldsymbol{\eta} - \mathbf{A}_\eta\mathbf{c})^{\mathrm{T}}(\boldsymbol{\eta} - \mathbf{A}_\eta\mathbf{c}) \\ &\quad + \mu^2(\mathbf{g} - \mathbf{A}_g\mathbf{c})^{\mathrm{T}}(\mathbf{g} - \mathbf{A}_g\mathbf{c}) \\ &= \alpha^2\mathbf{c}^{\mathrm{T}}\mathbf{c} + (\mathbf{d} - \mathbf{A}\mathbf{c})^{\mathrm{T}}(\mathbf{d} - \mathbf{A}\mathbf{c}). \end{aligned} \tag{10}$$

This is the formulation of a damped least-squares problem. Taking derivatives and equating to zero yields

$$\left(\mathbf{A}^{\mathrm{T}}\mathbf{A} + \alpha^2\mathbf{I}_m\right)\mathbf{c} = \mathbf{A}^{\mathrm{T}}\mathbf{d} \tag{11}$$

with $\mathbf{I}_m$ the identity matrix of order m, m being the number of data, which is also the order of the system. Provided that the coefficient matrix is symmetrical and positive definite, the solution can be achieved by Cholesky factorization. When a large number of stations is handled, the drawbacks are the m-order matrix multiplication $\mathbf{A}^{\mathrm{T}}\mathbf{A}$, and the inversion needed to solve the system. An alternative way of resolution is by applying the method of conjugate gradients (i.e. Pilkington 1997). This alternative does not require the construction of $\mathbf{A}^{\mathrm{T}}\mathbf{A}$, and even, if necessary, $\mathbf{A}$ itself, whose coefficients, expressed by eqs (4) and (5), can be evaluated every time they are employed.

After the source has been constructed, both geoidal heights and gravity anomalies can be evaluated at any desired location, for instance the points of a grid at a constant level.

TESTS ON SYNTHETIC DATA

Spherical earth model

From an irregular set of sources located at a uniform depth of 10 km, exact geoidal heights and gravity anomalies were computed at zero level, covering an area centred at 45°S latitude and arbitrary longitude, spanning 1° latitude and 1°30′ longitude. Both fields are contoured in Figs 2(a) and (b) respectively. Then, geoidal heights at 12 arbitrary points were chosen as 'measured geoid points', and gravity anomalies at 257 points as 'measured gravity points', and for the sake of comparison the exact geoid height which corresponds to each gravity observation was also calculated.

Then, using the method of this paper with only the 12 geoid values, a source was constructed whose effect provides a smoothed version of the actual geoid (Fig. 2c). When geoid undulations, from this model, are calculated at the gravity locations, the fit to the data is poor, with a root-mean square (rms) difference of 6.7 cm, and peaks of −19 and +25 respectively (Table 1). On the other hand, calculations performed including all geoid and gravity data, with small *a priori* standard deviations in eq. (11) (0.001 m for the geoid, 0.1 mGal for gravity, taking into account that data are exact, and depth factors 3 for the geoid and 2 for gravity), yield a source very different from the actual source because the masses lie at different depths. Yet, its geoid effect on the gravity stations differs very little from the actual geoid, the differences are of the order of the standard deviations considered. In other words, the incorporation of 257 gravity stations to the 12 geoid stations reconstruct the geoid almost exactly.

As a more realistic approach, data were contaminated with Gaussian noise of zero mean and a standard deviation compatible with usual measurements: 0.02 m for the geoidal heights and 2 mGal for gravity anomalies. Solving the problem from eq. (11) with those *a priori* standard deviations and the same depth to the sources, a solution was obtained (Fig. 2d and Table 1) that fits the geoid over the gravity stations with a mean quadratic error of 0.02 m and peak values of ±0.04 mGal, which is a very acceptable approximation compared with the geoid-only interpolations. Keeping the geoid precision in 0.02 m, and increasing the gravity noise to 4 mGal, the mean quadratic error rises to 0.03 m, which may still be acceptable (Table 1).

Planar model

With the same values at the stations, and converting geographical into rectangular coordinates simply by using the distances along the central arcs, the problem of predicting the geoid heights at the gravity stations was solved using a simplified planar model. The results obtained show no significant differences, and the predicted values fit the exact values (which were calculated from the curved model) within no larger standard deviations. It illustrates that for areas of the order considered here, the influence of curvature of the Earth is not a critical issue.

APPLICATION TO A REAL DATA SET

Perdomo & Del Cogliano (1999) presented a survey of GPS geoidal heights covering the whole Buenos Aires province of Argentina. This province encompasses most of the Pampean plains, with a nearly flat relief, and includes small ranges at its southern part. One hundred and eighty measurements were performed, of which 110, located at the nodes of the Argentine levelling network, are considered as principal points. The typical distance between them is 60 km, and the estimated accuracy of the ellipsoidal heights is about 1 to 2 cm. A map showing the location of the stations and the trend of the geoid anomalies they define is represented in Fig. 3(a).

On the other hand, a vast network of gravity measurements covers the area, mainly from the Military Geographic Institute of Argentina (IGM) and the national universities of La Plata and Buenos Aires. We chose a set of 789 of them, shown in Fig. 3(b) along with the free-air gravity contours. Thus, in order to construct the gravity-enhanced geoid map, we add those 789 gravity stations and determine an equivalent source with the following parameters: standard deviation of geoidal heights 0.01 m; standard deviation of gravity anomalies 2 mGal; standard deviation of the source values 1×10^6; depth factor under the geoid stations 3; depth factor under the gravity stations 2.

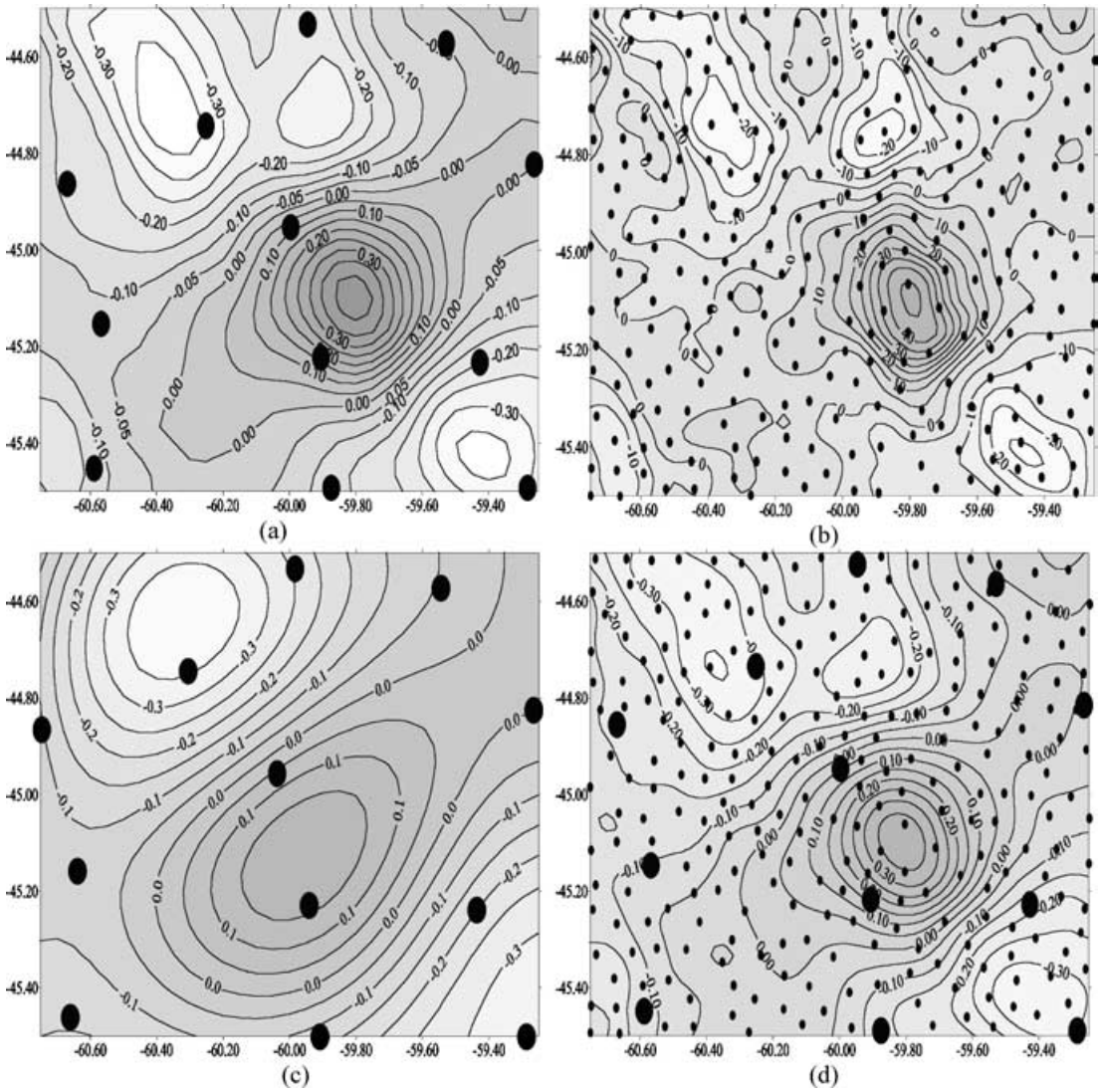

Figure 2. Tests on synthetic data. (a) Geoid undulations calculated from an irregular source, and location of the 12 stations used as geoid measurements. The contour interval is 0.05 m. (b) Gravity anomalies generated by the same source, and location of the 257 stations used as gravity measurements. The contour interval is 5 mGal. (c) Geoid interpolation from the 12 geoid measurements, without regard to the gravity values. The contour interval is 0.05 m. (d) Combined geoid interpolation using the 12 geoid plus the 257 gravity measurements, both contaminated with Gaussian noise. The contour interval is 0.05 m. Results compare well with the true undulations shown in part (a) (see also Table 1).

The *a posteriori* standard deviations after solving the system were of the order of the *a priori* estimates. The source produces the gravity-enhanced geoidal height map of Fig. 3(c), which differs from the map in Fig. 3(a) by up to about 0.2 m at some locations.

Fig. 4, within Buenos Aires province, with the same data and equivalent source, focuses on the area encompassing the Salado Basin. This is a major sedimentary basin with an unusual pattern of positive gravity anomalies (Bouguer and free-air anomalies are almost identical here due to the low elevation of the horizontal relief), and this feature has been interpreted by Introcaso & Ramos (1984) in terms of intruded magmatic materials which originated in a tri-radial rift. By comparing the maps in Fig. 4(b) (only geoid measurements)

Table 1. Tests on synthetic data. Geoidal heights calculated from a model are reconstructed on the basis of other geoid and gravity data points computed from the same model, incorporating Gaussian noise in some cases. rms and peak differences show the degree of fit achieved (see also Fig. 2).

Geoid		Gravity		Differences between interpolated and exact values		
Number of points	Noise (m)	Number of points	Noise (mGal)	rms	Negative peak	Positive peak
12	–	–	–	0.07	−0.25	0.19
12	–	257	–	0.00	−0.01	0.01
12	0.02	257	2.00	0.02	−0.03	0.02
12	0.02	257	4.00	0.03	−0.06	0.06

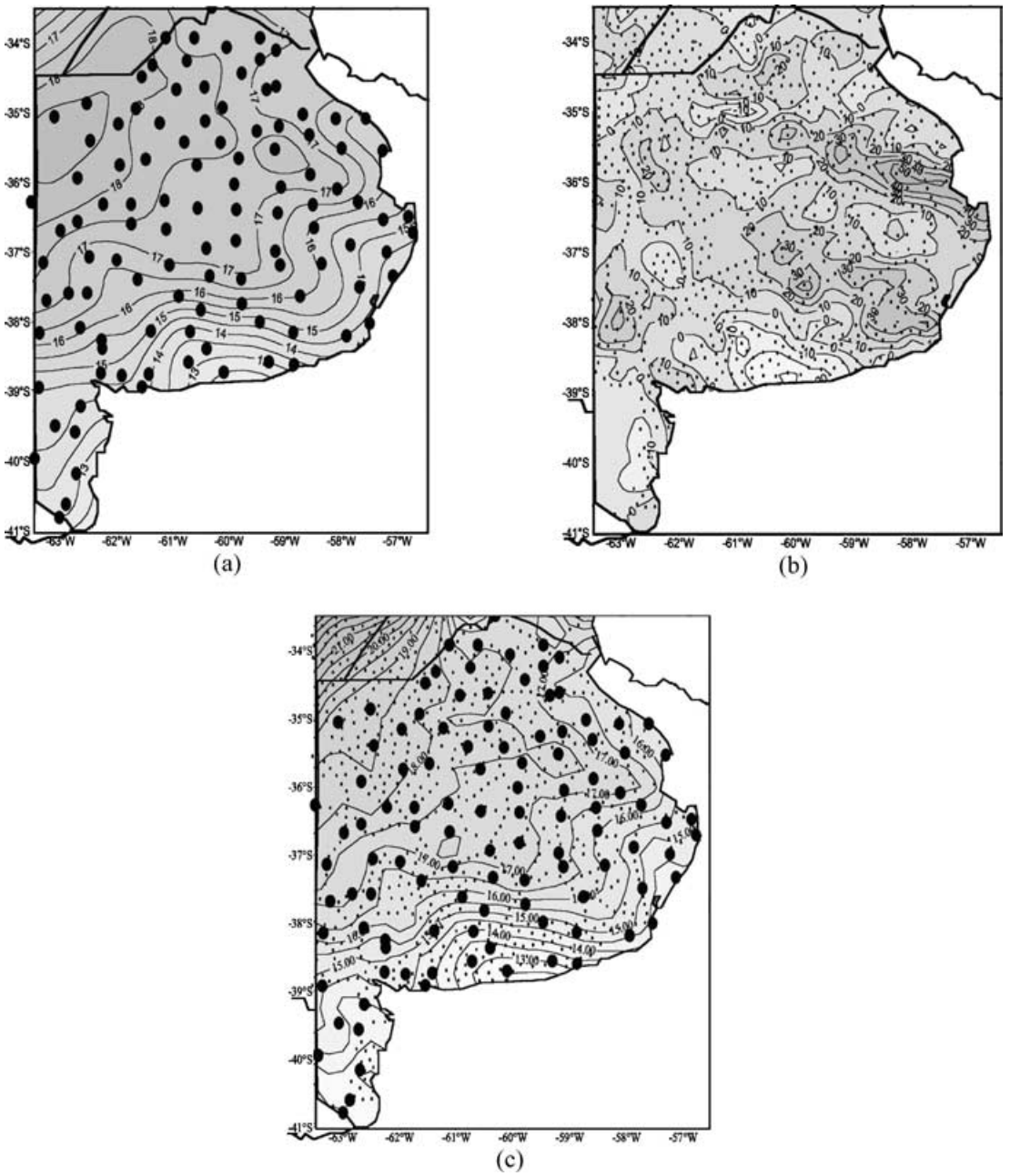

Figure 3. Application to a real data set. (a) Trend of the geoid undulations on Buenos Aires province, Argentina, obtained from 110 GPS measurements performed by Perdomo & Del Cogliano (1999). The contour interval is 0.5 m. (b) Map of free-air gravity anomalies on the same area, using 789 stations. The contour interval is 10 mGal. (c) Gravity-enhanced geoid map of Buenos Aires province, Argentina, which combines information from both GPS and gravity surveys by applying the technique developed in this paper.

and Fig. 4(c) (gravity-enhanced geoid), the differences in Fig. 4(d) illustrate how the inclusion of gravity influences the local features of the geoid. As a by-product, the geoid-enhanced gravity map at sea level of Fig. 4(e) is calculated from the same source that originates the gravity-enhanced geoid map, and shows the positive pattern of the anomaly.

CONCLUSIONS

Using a simultaneous inversion of potential and gravity anomalies into a two-layer equivalent source on the basis of a Bayesian criterion, gravity-enhanced geoid undulation charts may be constructed. A few GPS measurements on accurately levelled stations, considered as exact, are combined with denser sets of free-air gravity anomalies, enabling in this way the interpolation of the local features of the geoid by taking into account true geophysical information. No remove–restore steps are necessary, and the technique can be applied to either planar or spherical earth models without further complexity.

The synthetic and real case examples presented support the applicability of the technique to infer geoid elevations, and enhance the benefits of incorporating suitable *a priori* information to solve the problems dealt with.

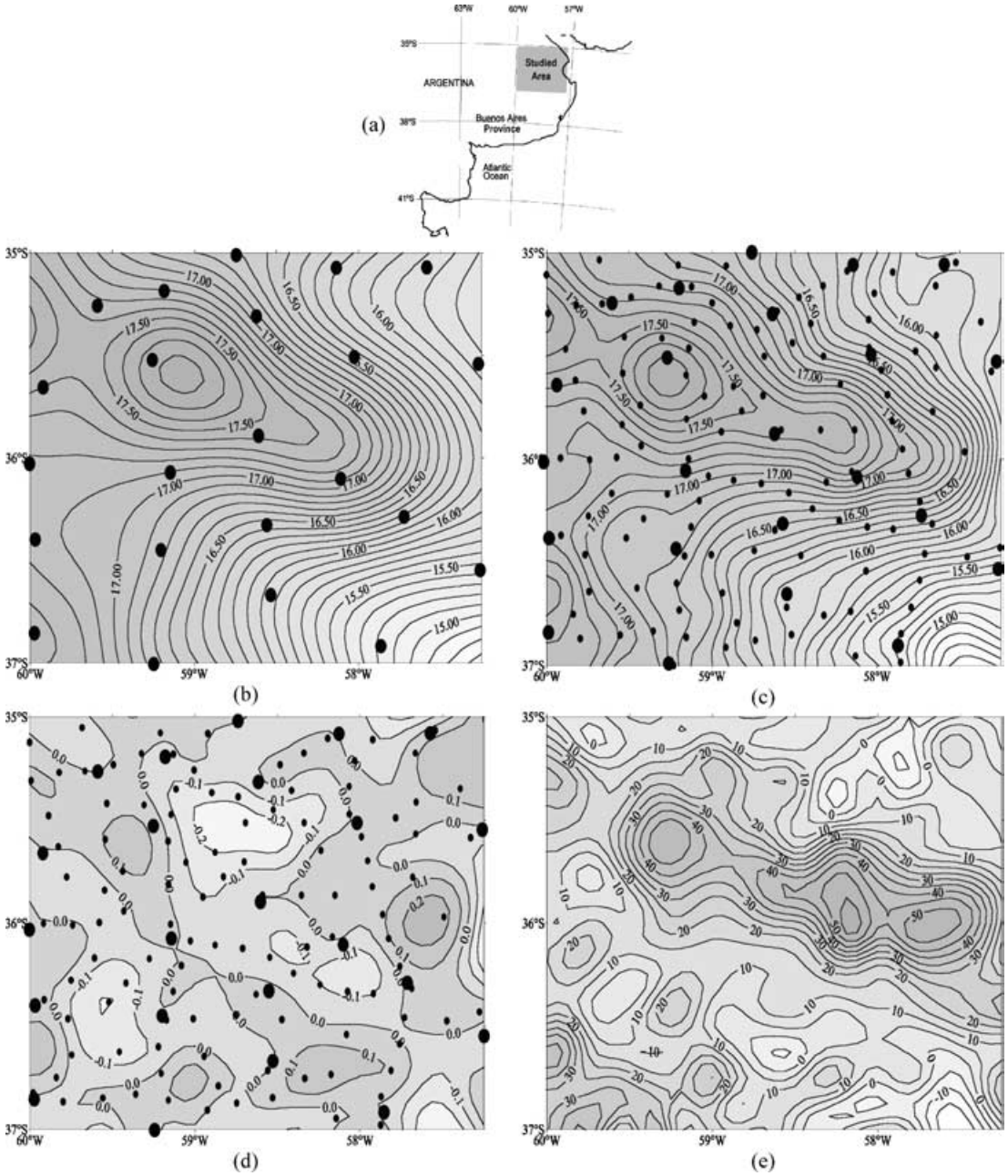

Figure 4. The Salado basin. Maps are magnifications of the maps in Fig. 3. (a) Location of the area. (b) Regional GPS geoid from Fig. 3(a). The contour interval is 0.1 m. (c) Gravity-enhanced geoid from Fig. 3(c). The contour interval is 0.1 m. (d) Differences between the gravity-enhanced and the regional geoid. Peaks exceed ±0.2 m. The contour interval is 0.1 m. (e) Combined free-air gravity map at sea level obtained as a by-product from the same equivalent source that generates the geoid map. The contour interval is 5 mGal.

ACKNOWLEDGMENTS

This work has been partially supported by PIP 03056 (Res. 1478/01), CONICET, Argentina.

REFERENCES

Antunes, C. & Catalao, J., 2000. On the comparison between point mass and collocation methods for geoid determination, in XXV General Assembly of the EGS, Session G7: Techniques for Local Geoid Determination, 25–29 April, Nice, France, http://correio.cc.fc.ul.pt/~mcarlos/poster00.pdf.

Arabelos, D. & Tscherning, C.C., 1998. The use of least squares collocation method in global gravity field modeling, *Phys. Chem. Earth,* **23,** 1–12.

Balmino, G., 1972. Representation of the Earth potential by buried masses, in *The Use of Artificial Satellites for Geodesy*, AGU Geophysical Monograph 15, pp. 121–124, eds Henriksen, S.W., Mancini, A. & Chovitz, B.H., American Geophysical Union, Washington, DC.

Cordell, L., 1992. A scattered equivalent-source method for interpolation and gridding of potential-field data in three dimensions, *Geophysics,* **57,** 629–636.

Dampney, C.N.G., 1969. The equivalent source technique, *Geophysics,* **34,** 39–53.

Gleason, D.M., 1990. Obtaining earth surface and spatial deflections of the vertical from free-air gravity anomaly and elevation data without density assumptions, *J. geophys. Res.,* **95,** 6779–6786.

Guspí, F., 1991. Rapid modeling and inversion of axisymmetric potential fields using equivalent sources, *Rev. Geofis.,* **47,** 19–26.

Guspí, F. & Introcaso, B., 2000. A sparse spectrum technique for gridding and separating potential field anomalies, *Geophysics,* **65,** 1154–1161.

Hansen, R.O. & Miyazaki, Y., 1984. Continuation of potential fields between arbitrary surfaces, *Geophysics,* **47,** 787–795.

Hauck, H. & Lelgemann, D., 1984. Regional gravity field approximation with buried masses using least-norm collocation, *Manuscr. Geodaet.,* **10,** 50–58.

Heiskanen, W.A. & Moritz, H., 1967. *Physical Geodesy*, W.H. Freeman, San Francisco.

Introcaso, A. & Ramos, V., 1984. La cuenca del Salado: un modelo de evolución aulacogénica, *Actas XI Congr. Geol. Argentino,* **3,** 27–46.

Lahmeyer, B., 1988. Gravity field continuation of irregularly spaced data using least squares collocation, *Geophys. J.,* **95,** 123–134.

Lehmann, R., 1993. The method of free-positioned point masses—geoid studies on the Gulf of Bothnia, *Bull. Geod.,* **67,** 31–40.

Lemoine, F. *et al.* , 1998. *The development of the joint NASA, CSFC and NIMA geopotential model EGM96*, NASA/TP–206861, Goddard Space Flight Center, Greenbelt, MD.

Levallois, J.J., 1962. Considérations générales sur les réductions de la pesanteur, *Bull. Geod.,* **63,** 79–93.

Li, X. & Goetze, H.J., 2001. Ellipsoid, geoid, gravity, geodesy, and geophysics, *Geophysics,* **66,** 1160–1668.

Moritz, H., 1980. *Advanced Physical Geodesy*, Wichmann Verlag, Karlsruhe.

Ockendon, J.R. & Turcotte, D.L., 1977. On the gravitational potential and field anomalies due to thin mass layers, *Geophys. J. R. astr. Soc.,* **48,** 479–492.

Perdomo, R. & Del Cogliano, D., 1999. The geoid in Buenos Aires region, *Int. Geoid Service,* **9,** 109–116.

Pilkington, M., 1997. 3-D magnetic imaging using conjugate gradients, *Geophysics,* **62,** 1132–1142.

Sacchi, M.D. & Ulrych, T.J., 1996. Estimation of the discrete Fourier transform, a linear inversion approach, *Geophysics,* **61,** 1128–1136.

Schwarz, K.P., Sideris, M.G. & Forsberg, R., 1990. The use of FFT techniques in physical geodesy, *Geophys. J. Int.,* **100,** 485–514.

Torge, W., 2001. *Geodesy*, 3rd edn, W. de Gruyter, Berlin.

Tscherning, C.C., Knudsen, P. & Forsberg, R., 1994. *Description of the GRAVSOFT Package*, Technical Report, Geophysical Institute, University of Copenhagen

Ulrych, T.J., Sacchi, M.D. & Woodbury, A., 2001. A Bayes tour of inversion: a tutorial, *Geophysics,* **66,** 55–69.

Volgyesi, L., 2001. Local geoid determinations based on gravity gradients, *Acta Geodaet. Geophys. Hung.,* **36,** 153–162.

Xia, J. & Sprowl, D.R., 1991. Correction of topographic distortions in gravity data, *Geophysics,* **56,** 537–541.

Zeyen, H. & Pous, J., 1991. A new 3-D inversion algorithm for magnetic total field anomalies, *Geophys. J. Int.,* **104,** 583–591.